Computational Neuroscience

Trial time warping to discriminate stimulus-related from movement-related neural activity

Oswaldo Perez [a], Robert E. Kass [b,c,d], Hugo Merchant [a,*]

[a] Instituto de Neurobiología, UNAM, Campus Juriquilla, Mexico
[b] Center for the Neural Basis of Cognition, Carnegie Mellon University, United States
[c] Machine Learning Department, Carnegie Mellon University, United States
[d] Department of Statistics, Carnegie Mellon University, United States

HIGHLIGHTS

▶ A warping method is used to determine best alignment of cell responses to events.
▶ Bayes factors are used to classify sensory or motor neurons.
▶ Movement times, firing rate and duration of response are critical in the analysis.

ARTICLE INFO

ABSTRACT

In tasks where different sensory, cognitive, and motor events are mixed in a sequence it is difficult to determine whether neural activity is related to any behavioral parameter. Here, we consider the case in which two alternative trial-alignment schemes correspond to two different neural representations, one stimulus-related and the other movement-related, using both simulations of neural activity and real recordings in the medial premotor areas during a multiple-interval tapping task called synchronization-continuation task (SCT). To discover whether neural responses are better aligned to sensory or motor events we introduce a family of trial-alignment time-warping functions indexed by a single parameter such that when the parameter takes the value 0 the trials are aligned to the stimulus and when the parameter takes the value 1 they are aligned to the movement. We then characterize neurons by the best-fitting alignment scheme (in the sense of maximum likelihood) under the assumption that the correct alignment would produce homogeneous trials without excess trial-to-trial variation. We use Bayes factors to determine the evidence in favor of sensory or motor neural alignments. The simulations revealed that the variability in neural responses and sequential motor outputs are key parameters to obtain appropriate warping results. In addition, the analysis on the activity of 500 neurons in the medial premotor areas of monkeys executing the SCT showed that most of the neural responses (54.2%) were aligned to the tapping movements instead of the stimuli used to drive the temporal behavior.

© 2012 Elsevier B.V. All rights reserved.

1. Introduction

The mammalian cerebral cortex has the ability to construct dynamic neuronal representations about sensory events, forthcoming movements, and a myriad of cognitive processes that link sensation to motor execution. Cortical responses in sensory areas show short onset latencies to the presentation of stimuli (Mountcastle et al., 1990; Romo et al., 1996; Nowak et al., 1995; Liang et al., 2002), whereas motor areas show sharp activation profiles before movement onset (Georgopoulos et al., 1982; Crutcher and Alexander, 1990). In contrast, the responses in association areas are less tightly locked to sensory, cognitive, or motor events (Mountcastle et al., 1975; Merchant et al., 2004; Chafee et al., 2007). The picture gets more complicated when we consider that the activity in the cortex exhibits a considerable amount of trial-to-trial variability. In fact, both the shape of the activation profile (Shadlen and Newsome, 1998; Lee et al., 1998; Averbeck et al., 2006a) and the onset latency (Merchant et al., 2001; Nawrot et al., 2003) show different levels of variability across cortical areas for the diverse behavioral aspects of a specific paradigm. Therefore, a critical problem in the cortical physiology of behaving animals is to determine

whether the response of neurons is related to the different aspects of a task. Different algorithms have been implemented to determine the onset latency of neurons using parametric (Ellaway, 1978; Seal et al., 1983; Davey et al., 1986; Baker and Gerstein, 2001) or nonparametric methods (Sanderson, 1980; Nawrot et al., 2003; Ventura, 2004). Most of these methods take into account the trial-to-trial variability of neuronal activity and can determine with different levels of accuracy the onset response latency, especially to sensory stimuli. However, these methods are not designed to test whether the activity of a cell is associated to the sensory, cognitive, or motor aspects of a task, particularly when the task includes many such events in a sequence.

Here we describe a novel warping method to discover whether the cell responses are better aligned to the sensory or motor events of the synchronization-continuation tapping task (SCT). In this task monkeys synchronize their tapping with pacing isochronous auditory stimuli for a number of intervals, and then continue tapping at the instructed rate without the advantage of the sensory metronome (Repp, 2005; Wing and Kristofferson, 1973). We simulated activity during the four stimuli and four taps of the synchronization phase of the SCT, and restricted the analysis of the recorded neural responses to those cells that showed activity modulations during this task phase (Zarco et al., 2009; Merchant et al., 2011). Every analysis of multi-trial spike-train data begins by introducing some form of temporal alignment across trials. Here, we initially align the trials to the stimuli and write the resulting temporal alignment as a function $[T_0(t)]$. We next let $[T_1(t)]$ be the temporal alignment corresponding to movement and we introduce weighted combinations of these two extreme cases to obtain intermediate alignment schemes $[T_w(t)]$ indexed by a weight parameter $[w]$. We then assume that under the correct alignment the trials will be homogeneous, without excess trial-to-trial variability above that predicted by a Poisson process with a time-varying firing intensity function, and we proceed to find the best-fitting alignment scheme. Finally, for each neuron, we used Bayes factors to evaluate evidence in favor of a sensory or motor alignment (Kass and Raftery, 1995). We found in the simulations that the inter-trial variability of the tapping movements, as well as the magnitude and duration of the neural activity associated to sensory or motor events are critical parameters to obtain proper warping values. Furthermore, the results showed that most neurons in the medial premotor areas of monkeys executing the SCT were aligned to the tapping movements instead of the stimuli used to drive the temporal behavior. We conclude that the present method can be used reliably in a variety of behavioral paradigms where multiple, sensory, motor, and/or cognitive events are intermixed in a sequence, in order to determine to which event the cell responses are better aligned.

2. Materials and methods

2.1. Animals

Two male monkeys (*Macaca mulatta*, 5–7 kg BW) were trained to tap on a push button in the SCT. Neurophysiological recordings were carried out in the MPC during performance of the task using a system with 7 independently movable microelectrodes (1–3 MΩ, Uwe Thomas Recording, Germany, see Merchant et al., 2011). Single-unit activity was extracted from these recordings using the Plexon off-line sorter (Plexon, Dallas, TX). All the animal experimental procedures were approved by the National University of Mexico Institutional Animal Care and Use Committee and conformed to the principles outlined in the Guide for Care and Use of Laboratory Animals (NIH, publication number 85-23, revised 1985).

2.2. Synchronization-continuation task (SCT)

The SCT used in this study has been described before (Merchant et al., 2008; Zarco et al., 2009). Briefly, the monkeys were required to push a button each time stimuli with a constant interstimulus interval were presented, which resulted in a stimulus–movement cycle. After four consecutive synchronized movements, the stimuli were eliminated, and the monkeys continued tapping with the same interval for three additional intervals. Monkeys received a reward if each of the intervals produced had an error < 35% of the target interval. Trials were separated by a variable inter-trial interval (1.2–4 s). The target intervals, defined by brief auditory (33 ms, 2000 Hz, 65 dB) stimuli, were 450, 550, 650, 850, and 1000 ms, and were chosen pseudo-randomly within a repetition. Five repetitions were collected for each target interval. For the warping analysis we only used the data of the four stimuli and their corresponding tapping movements of the synchronization phase of the task. We analyzed 500 neurons that showed a minimum discharge rate of 4 Hz and showed task related activity based on an ANOVA where the discharge rate was the dependent variable and the task epoch (initial control key holding period [500 ms] vs. the synchronization phase) was the factor.

2.3. Time warping

In this work, we propose a warping transformation (Wang and Gasser, 1999) to determine whether the activity of a cell was better aligned to sensory or motor events during the SCT. We defined the time of sensory events as the instant in which the auditory stimulus was presented. The time of motor events was defined as the moment in which the monkey tapped on the button. Hence, we only used the behavioral information and cell activity recorded during the synchronization phase of the SCT. The goal of this analysis was to find the cell alignment that produced the smallest intertrial variability. The method has the following steps:

(1) The action potential times $\{t_{i,j}\}$ were initially aligned to the stimulus times $\{S_{i,1}, S_{i,2}, S_{i,3}, S_{i,4}\}$, where i correspond to the trial repetition and j to the spike number. In addition, we defined the following transformation in order to align the action potential times $\{t_{i,j}\}$ to the motor events $\{M_{i,1}, M_{i,2}, M_{i,3}, M_{i,4}\}$:

$$T_i(t) = \frac{L_{j+1} - L_j}{M_{i,j+1} - M_{i,j}}(t - M_{i,j}) + L_j \quad \text{when} \quad M_{i,j} \leq t \leq M_{i,j+1} \quad (1)$$

and $\{L_1, L_2, L_3, L_4\}$ were landmark references. L_1 was the average reaction time of the monkeys for the first stimulus during cell recordings, whereas L_2 to L_4 were defined as the target interval duration (i.e. 450, 550, and 650 ms). This transformation was performed for each trial across the five interval durations in the SCT.

(2) The warping transformation was:

$$T_w^i(t) = wT_i(t) + (1 - w)t \quad (2)$$

that depended on the parameter w. When $w = 0$ the responses were aligned to the sensory events S. When $w = 1$ the responses were aligned to the motor events M. w values between 0 and 1, in steps of 0.1, produced alignments between S and M events.

(3) The average spike density function $r_w(t)$ for every interval duration across trials was computed using the following equation for a particular w.

$$r_w(t) = \frac{1}{N} \sum_{i=1}^{N} \sum_{j=1}^{n_i} \frac{1}{\sqrt{2\pi}\sigma} e^{-\frac{(t - T_w^i(t_{i,j}))^2}{2\sigma^2}} \quad (3)$$

γ_1	Evidence in favor of motor category
0 to 1/2	Bare mention
1/2 to 1	Substantial
1 to 2	Strong
>2	Decisive

where n_i is the total number of action potentials in a trial i, N is the total number of trials, and the Gaussian kernel width $\sigma = 20$ ms.

(4) The likelihood function representing the multi-trial response variability of a cell, for a particular w alignment, was calculated assuming that $D_i = \{t_{i,1}, t_{i,2}, \ldots, t_{i,n_i}\}$, the times of n_i spikes in trial i, is a non-homogeneous Poisson process with rate $r_w(t)$:

$$L_i(w) = p(D_i|w) = e^{-\int_0^T r_w(t)dt} \prod_{j=1}^{n_i} r_w(t_{i,j}) \tag{4}$$

Since the likelihood function represents the multi-trial response variability of a cell using the average spike density function, we used a leave-one-out cross-validation method to determine the variability of trial i from the average firing rate. Then, for every neuron, we computed the total probability that was the product of $L_i(w)$ for every trial i and for each of the 5 target interval durations Int:

$$L(w) = \prod_{Int} \prod_i L_i(w) \tag{5}$$

Finally, we found the w that maximized the function $L(w)$, which corresponds to the value that maximizes the spike prediction accuracy across trials and that was called warping value ($\hat{w}$). This measure is associated with the warping value that minimizes the intertrial variability of the cell activity.

2.4. Bayes factor

The warping transformation finds the best-fitting alignment of a cell. However, it is important to determine the probability of assigning a particular warping value to a sensory or motor alignment. Let D be the set of all spike times of a neuron across trials and interval durations. For each cell we have:

$$\begin{aligned} p(D|sensory) &= L(0) \\ p(D|motor) &= L(1) \\ p(D|complex) &= \int_0^1 L(w)dw \end{aligned} \tag{6}$$

We then we define the following Bayes factors:

$$\begin{aligned} \gamma_1 &= \log_{10}\left(\frac{p(D|motor)}{p(D|sensory)}\right) \\ \gamma_2 &= \log_{10}\left(\frac{p(D|motor)}{p(D|complex)}\right) \\ \gamma_3 &= \log_{10}\left(\frac{p(D|sensory)}{p(D|complex)}\right) \end{aligned} \tag{7}$$

These factors summarize the evidence provided by the data in favor of one category, namely, motor (if $\gamma_1 > 0$ and $\gamma_2 > 0$), sensory (if $\gamma_1 < 0$ and $\gamma_3 > 0$), and complex (if $\gamma_2 < 0$ and $\gamma_3 < 0$).

Adapting the strength of evidence in favor of a category given by Kass and Raftery (1995) to the present problem, the classification strength using γ_1 to discriminate motor cells is given in Table 1.

We classified the cells in three different categories based on this information as follows: motor-neuron if $\gamma_1 > 1$ and $\gamma_2 > 1$, sensory-neuron if $\gamma_1 < -1$ and $\gamma_3 > 1$, and complex-neuron if $\gamma_2 < -1$ and

$\gamma_3 < -11$. Cells that did not meet any of the criteria for classification were considered indeterminate. Therefore, the γ thresholds used in the present paper (a value larger than 1) provide strong evidence in favor of a particular cell category, according to Table 1.

2.5. Spike-train simulations

In order to investigate how the properties of the cell activation profiles and the behavioral performance affected the warping analysis and the corresponding gamma values, we generated random spike-trains as well as behavior. In particular, we checked how the following key parameters affected the power (see Fig. 2):

(a) We set the stimulus times $\{S_1, S_2, S_3, S_4\}$ using an intertrial stimulus interval of 650 ms.

(b) We generated random movement events $\{M_{i,1}, M_{i,2}, M_{i,3}, M_{i,4},\}$, where i correspond to simulation trial, from a Gaussian distribution with mean $\{L_1, L_2, L_3, L_4,\}$ and standard deviation σ_M. In this case $Lj = Sj + \overline{RT}$, where $\overline{RT}$ is the average reaction time of animals (360 ms).

(c) We generated spike-trains from a non-homogenous Poisson process with rate

$$r_i(t) = \begin{cases} M_R & \text{if } \mu_j - \dfrac{\sigma_R}{2} \leq t \leq \mu_j + \dfrac{\sigma_R}{2} \\ 0 & \text{otherwise} \end{cases} \tag{8}$$

for all j, where:

$$\mu_j = w_{simul}L_j + (1 - w_{simul})S_j + \tau_R(1 - 2w_{simul}) \tag{9}$$

μ_j depended on value w_{simul} that corresponds to the simulated warping alignment. τ_R was the onset response latency of the cell with respect to the w_{simul}.

We used the inverse $(T^i_{w_{simul}})^{-1}(t)$ on the generated spike-trains to return to original time scale (aligned to stimulus times). To this end, initially we mixed Eqs. (1) and (2) to have:

$$T^i_w(t) = A(t - M_{i,j}) + B \quad \text{when} \quad M_{i,j} \leq t \leq M_{i,j} \tag{10}$$

where $A = (w(L_{i,j+1}) + (1 - w)(M_{i,j+1} - M_{i,j}))/(M_{i,j+1} - M_{i,j})$ and $B = wL_{i,j} + (1 - w)L_{i,j+1}$.

Then, the inverse warping transformation is given by:

$$(T^i_w)^{-1}(t) = \frac{t - B}{a} + M_{i,j} \quad \text{where } wL_{i,j} + (1 - w)M_{i,j} \leq t \leq wL_{i,j+1} \\ + (1 - w)M_{i,j+1} \tag{11}$$

(d) Finally, we calculated $\hat{w}$ and γ_1, γ_2 and γ_3 for 500 spike-train simulations that varied systematically across the following parameters: (1) the w_{simul} aligned value, (2) the standard deviation of movement events σ_M, (3) the response duration σ_R, (4) the mean firing rate M_R of the simulated neural responses, and (5) the onset response latency τ_R of the spike-trains (Fig. 2). Therefore, these simulations allowed for the systematic characterization of the effects of the cell activation profiles and the variability in the movements during the SCT task on the $L(w)$ function and the Bayes factors, in order to suggest practical guidelines to other studies using these methods.

(e) The parameters σ_R, M_R, τ_R, and σ_M were also estimated from the neurophysiological experiment as follows. σ_M was calculated as the standard deviation of movement times performed by the monkeys. For the neural parameters, first, we aligned the neural responses to $\hat{w}$. Then, we defined the response window for each trial and interval produced in the sequence as the interval between the first and last spikes. σ_R was the average of all response windows, whereas M_R was the corresponding
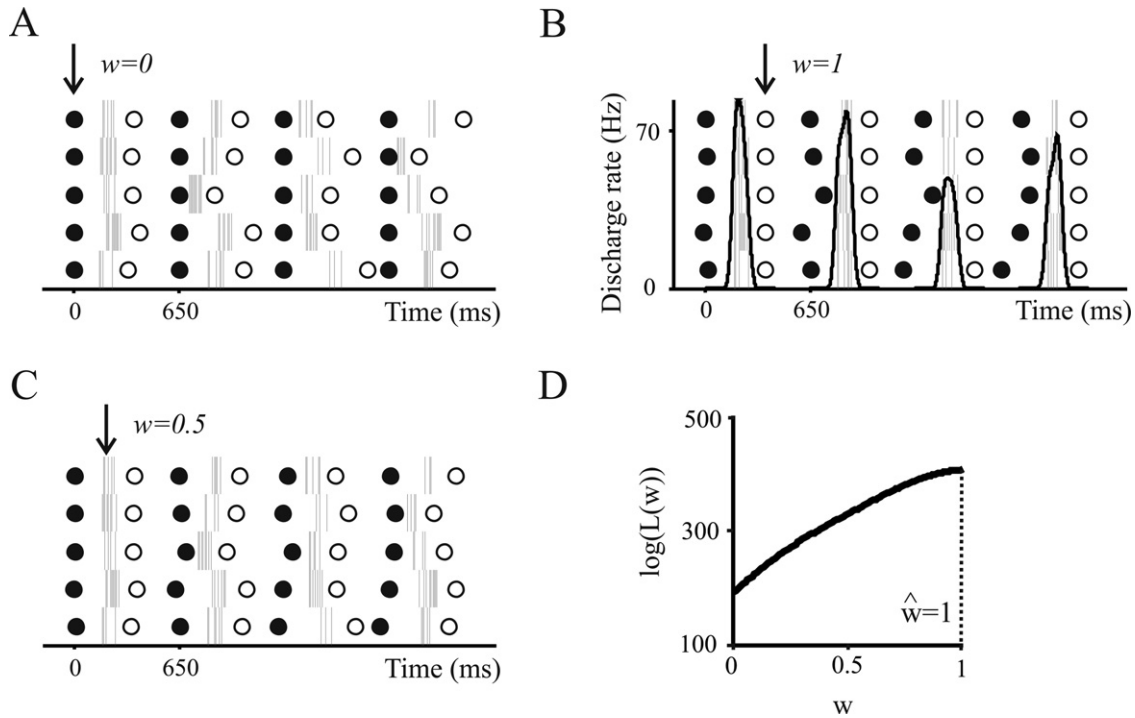
Fig. 1. Simulated spike-trains of a motor cell during the synchronization phase of the SCT. (A) Raster plot of the simulated activity aligned to the stimulus presentations (filled circles) with an interstimulus interval of 650 ms, where every tick mark corresponds to a single spike time stamp. (B) The same responses in A, but aligned to the button press (open circles) using the transformation in Eq. (1). The average spike density function (Eq. (3)) is shown in black. (C) The same response aligned of $w = 0.5$ using the warping transformation of Eq. (2). (D) The logarithm of the homogeneity measure $log(L(w))$, computed from Eq. (5), is plotted as a function of the warping value. The larger warping value (w^-) is equal to 1. A spline filter was used for smoothing the original data.

average firing rate. Finally, τ_R was the distance between $\widehat{w}$ and the beginning of the response window.

3. Results

3.1. Warping value

The SCT includes a sequence of sensory and motor events. We developed a transformation that allowed us to align spike times to the push-button events in a trial (see Section 2). This transformation depends on a parameter w which can acquire values between 0 and 1. When $w = 0$, spikes are completely aligned to the stimuli, as the original data. An example of this alignment is shown for simulated spike-trains in Fig. 1A (filled circles). Conversely, when $w = 1$, spike-trains are aligned to the motor events, as shown in Fig. 1B (open circles). Obviously, when responses were given intermediate w values, they were aligned between sensory and motor events, as depicted in Fig. 1C for $w = 0.5$. In order to find which w value was the best to minimize the intertrial variability for a given cell, we used a homogeneity measure, L, whose value was inversely proportional to this variability (see Section 2). Fig. 1D shows the $log(L(w))$ as a function of w for simulated spike-trains shown in Fig. 1A–C, where it can be seen that the highest probability is reached when $\widehat{w} = 1$. This means that the best alignment for the responses of this simulated response was to motor events.

3.2. Bayes factors

The warping value ($\widehat{w}$), which is the w value that maximize the $L(w)$ function, can be used to classify neurons as follows: cells with a warping value close to zero were considered as sensory; a motor neuron was a cell with a warping value close to 1; finally, cells with warping values between 0 and 1 were considered as complex cells (see Section 2). However, to determine how strong was

the evidence in the L probabilities described in Eq. (5) in favor of one response category we used the factors described in Eqs. (6) and (7) as discrimination parameters. Using the criteria provided by Kass and Raftery (1995) and described in Table 1, we classified
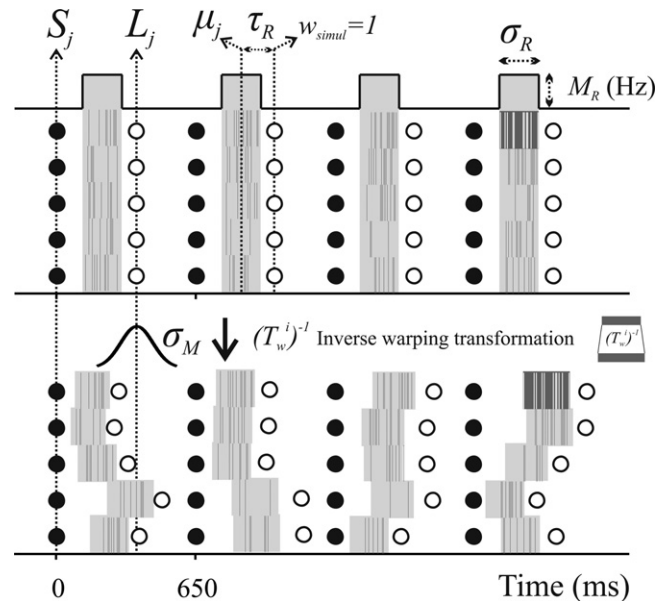
Fig. 2. Key parameters of the simulated spike-trains for the warping analysis. The standard deviation of movement events σ_M, the neural response duration σ_R, the maximum firing rate M_R of the simulated neural responses, and the onset response latency τ_R with respect to w_{simul} are shown. The top panel shows the spike trains generated from non-homogeneous Poisson process using Eq. (8). The bottom panel shows how the inverse warping transformation (Eq. (10)) is used to simulate the variability in the movement times (σ'_M) and to produce the spike-train alignments to the w_{simul}. The inset between panels shows the comparison of the σ_R of the darker gray response window in the top right between the original and warped spaces.
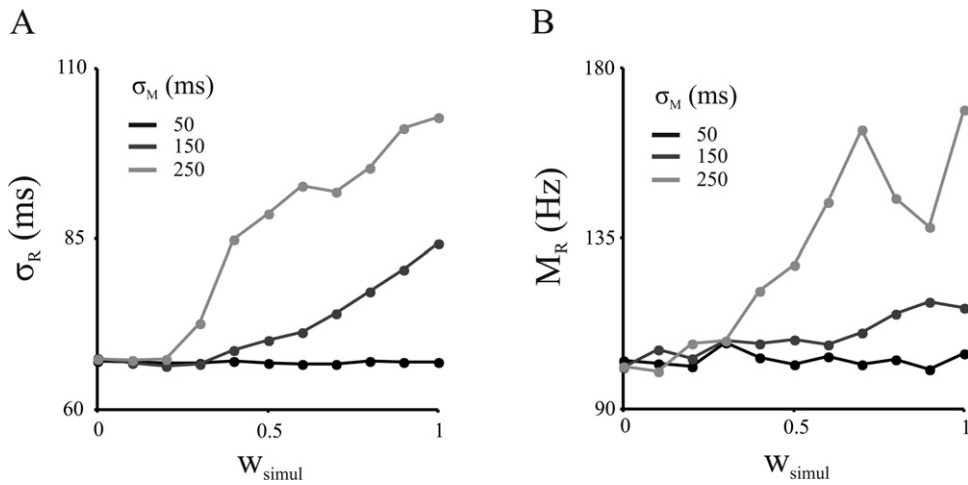
Fig. 3. (A) σ_R as a function of w_{simul} the three specified values of σ_M in the inset. (B) M_R as a function of w_{simul} the same σ_M values. Note the large increase in both σ_R and M_R as a function of w_{simul} for larger values of σ_M.

each cell into the three different categories using the following γ thresholds: motor when $\gamma_1 > 1$ and $\gamma_2 > 1$, sensory when $\gamma_1 < -1$ and $\gamma_2 > 1$, and complex when $\gamma_2 < -1$ and $\gamma_3 < -1$. Otherwise the cells were categorized as indeterminate.

3.3. Spike-train simulations

We simulated cell responses and behavioral events for five trials during the synchronization phase of the SCT in order to determine how different parameters affect the $log(L(w))$ function and the Bayes factors. These parameters include the mean (M_R), duration (σ_R), and onset response latency (τ_R) of the simulated spike-trains,

as well as the intertrial-variance or the movement responses of the subject (σ_M) (Fig. 2). We used a target interval of 650 ms between stimuli. These simulations depended on a parameter w_{simul} which also can acquire values between 0 and 1 (see Section 2). Fig. 3 shows that σ_R and M_R increased as a function of w_{simul} when applied the inverse warping transformation, particularly for high values of σ_M which produced elongated warping times. Furthermore, Fig. 4A shows the $log(L(w))$ function for simulated responses using different w_{simul}, where is evident the value $\hat{w}$ varies linearly as a function of w_{simul}. In addition, Fig. 4B shows how the three Bayes factors change as a function of w_{simul}. Both γ_1 and γ_2 show a monotonic increase, whereas γ_a shows a monotonic decrease as w_{simul} acquires
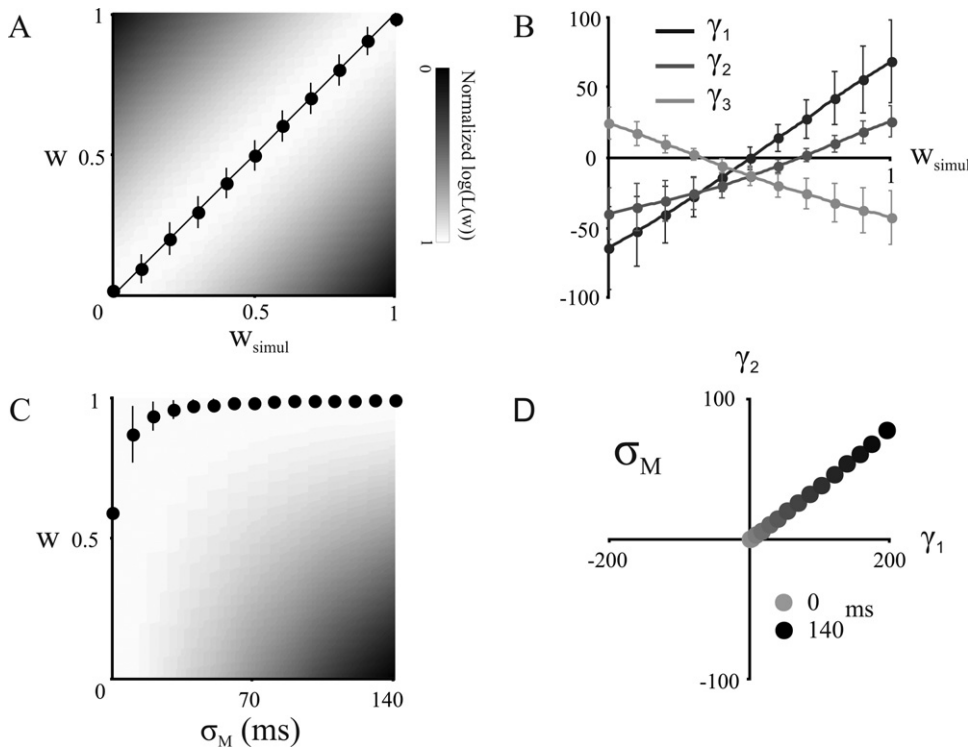
Fig. 4. (A) Normalized logarithm of the homogeneity measure $log(L(w))$ (gray scale) is plotted as a function of w and w_{simul} for simulated spike-trains with $\sigma_M = 70$ ms, $\sigma_R = 100$ ms, $M_R = 60$ Hz and $\tau_R = 150$ ms. Dots represent the average warping value $\hat{w}$ as a function of w_{simul} and the error-bars correspond to the standard deviation of 500 simulations. (B) γ_1 (black), γ_2 (dark gray) and γ_3 (light gray) as a function of w_{simul} for simulated spike-trains. Error-bars correspond to the standard deviation. The other parameters as (A). (C) Normalized $log(L(w))$ as a function of parameter σ_M for simulated spike-trains with $w_{simul} = 1$. Error bars are half a standard deviation. The other parameters as (A). (D) Average γ_1 against the γ_2 across the σ_M values depicted in (C). Color code in the inset.
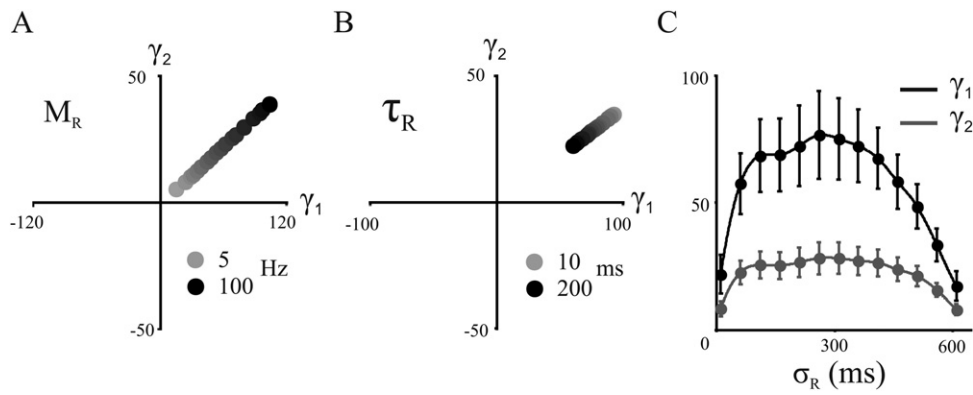
Fig. 5. Plots of γ_1 against the γ_2 for simulated spike-trains generated with $w_{simul} = 1$, $\sigma_M = 70$ ms, $\sigma_R = 100$ ms, $M_R = 60$ Hz and $\tau_R = 150$ ms but varying systematically across parameters: M_R (A) and τ_R (B) and σ_R (C). Conventions as in Fig. 4D.

values from 0 to 1 (Fig. 4B). Hence, as the w_{simul} becomes closer to 1 more evidence there is in the $log(L(w))$ function and the Bayes factors of a motor alignment. Next, we generated motor spike-trains ($w_{simul} = 1$), and found that as σ_M increases, the $log(L(w))$ function becomes more steep (Fig. 4C) and the corresponding γ_1 and γ_2 values increase (Fig. 4D). These results indicate that when the motor responses of the subject have an intertrial variability above 11 ms, the Bayes factors show decisive evidence for the motor alignment, as described in Table 1, for a γ_1 and γ_2 values larger than 2. In addition, we found that γ_1 and γ_2 values decrease as a function of M_R (Fig. 5A). The onset response latency (τ_R) of the simulated spike-trains has little effect on the γ values (Fig. 5B). Finally, the γ_1 and γ_2 values show large values for response durations (σ_R) between 60 and 460 ms, with sharply decreasing values below or above this range (Fig. 5C). To summarize, when the parameters of an experiment fall inside the following ranges, we know

that our warping method obtains appropriate results: $\sigma_M > 11$ ms, $M_R > 2$ Hz, and σ_R between 60 and 460 ms. Fortunately, these values encompass a wide range of cell responses and motor variability values, which include most of the neurophysiological data of cortical areas.

3.4. Neural recordings during the SCT

Next, we performed the warping analysis on MPC neurons of monkeys performing the SCT. Fig. 6 shows the response of three cells aligned to the motor events ($w = 1$; top of panels A–C). The corresponding values of σ_M, σ_R, τ_R, and M_R are depicted at the top. In addition, $log(L(w))$ as a function of w are illustrated at the bottom for each cell, where it can be seen that the highest probability is reached when $\hat{w} = 1$. This means that the best alignment for the responses of these cells was to motor events.
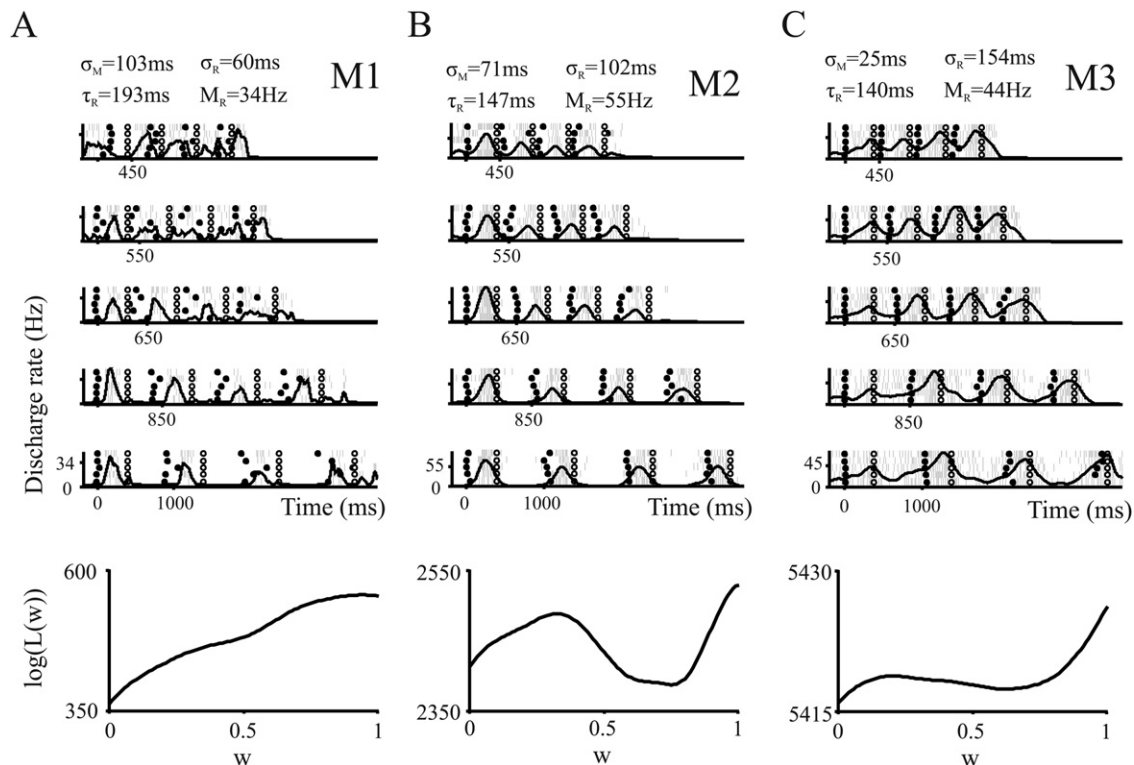
Fig. 6. Neural activity of three motor neurons (M1, M2, M3) during the SCT. Top panel shows the raster plots of the cells aligned to the button press and bottom panel is the logarithm of homogeneity measure $log L(w)$ as a function of w. For each neuron, the larger warping value (w^-) is equal to 1. See how the shape of the $log L(w)$ function can be influenced by parameters σ_M, σ_R, τ_R, and M_R depicted at the top. Conventions as in Fig. 1A.

Table 2
Number of cells that were classified as motor, sensory, complex and undetermined based of their γ values.

Category	Motor	Sensory	Complex	Indeterminate
Number of neurons	271	153	35	41
Percentage	54.2	30.6	7	8.2

The results of the Bayes factors analysis on our database, depicted in Table 2, shows that most of the neurons (271/500, 54.2%) recorded in MPC during the synchronization phase of the SCT were classified as motor. In addition, Fig. 7A shows the γ_1 and γ_2 values for the population of recorded neurons. Each dot represents a single neuron, where black dots represent the cells classified as motor and open dots represent the non-motor cells. The cells M1, M2, and M3 of Fig. 6 are marked with a white asterisk in Fig. 7A, and were categorized as motor. Furthermore, Fig. 7B depicts the γ_1 and γ_2 values for the same population of neurons. In this case black dots represent cells classified as sensory and open dots represent the non-sensory cells. Finally, Fig. 7C shows the strong correlation between the duration of the activation period (σ_R) and the mean discharge rate (M_R) of the recorded cells.

4. Discussion

We presented a method to determine whether the activity of a neuron was better aligned to sensory or motor events during the SCT, using a warping algorithm. This warping method not only realigned the trial-by-trial cell activity to the stimuli ($w = 0$) or to the button-press ($w = 1$), but also a wide range of intermediate values ($w > 0$ and $w < 1$). A maximum likelihood estimator was used to find the warping value that minimized the trial-by-trial variability, assuming that the activity of a cell was functionally associated with the behavioral parameter that produced the lowest intertrial variability. Then, a cell was categorized as sensory, complex, or motor based on Bayes factors that evaluate the evidence in favor of each alignment (Kass and Raftery, 1995). Spike-train simulations revealed that Bayes factors become larger when the magnitude of the neural response become larger, the inter-trial variability of the cell activity becomes smaller, and the variability motor responses of the subject becomes larger. In addition, the Bayes factors show a similar value for a wide range of cell response durations. Indeed, when the parameters of an experiment fall inside the following ranges: $\sigma_M > 9.6$ ms, $M_R > 5$ Hz, and σ_R between 60 and 460 ms, our warping method will obtain appropriate results. On the other hand, the fact that 54% of cells in MPC showed a significant alignment to the tapping movements during the SCT, while only 31% were aligned to sensory features, indicates that this premotor region is biased toward temporal processing in motor rather than in sensory terms.

The proposed method is applicable not only to the SCT, that has been a backbone in the timing literature (Repp, 2005; Wing and Kristofferson, 1973), but also to other sequential paradigms where there are more than one sensory, motor and/or cognitive events inside a trial. The study of the neurophysiological basis of sequential behavior has advanced enormously during the last ten years (Nakamura et al., 1998; Tanji, 2001; Lee and Quessy, 2003; Averbeck et al., 2006b). Neural signals encoding the ordinal and spatial elements of movement sequences have been described in diverse frontal areas during skeletomotor or oculomotor tasks. Nevertheless, these studies did not characterize whether the cell responses, associated with the sequential elements of the tasks, were aligned to the sensory or motor events of such paradigms. Our warping method could be used easily on such databases to get a reliable and fast answer in this regard. In addition, the proposed warping method could be used when predicting neural responses
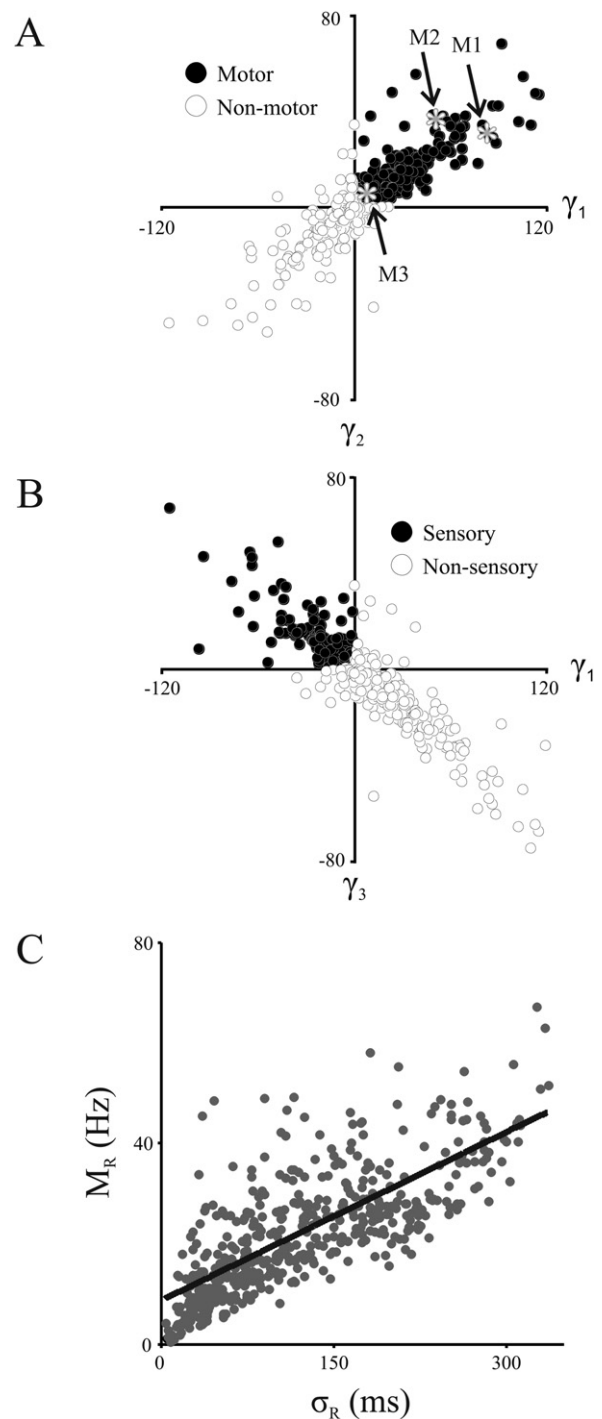
Fig. 7. (A) Plot of the γ_1 against the γ_2 for all neurons recorded in MPC. Each circle represents a cell. The upper right quadrant, where $\gamma_1 > 0$ and $\gamma_1 > 0$ is associated with the motor cells, whereas the other three quadrants define the cells that are non-motor, namely sensory or complex. The motor cells are displayed as filled circles, whereas open circle correspond to non-motor cells. The motor cells illustrated in Fig. 6 are shown as M1, M2 and M3 with a white asterisk. (B) Plot of the γ_1 against the γ_3. The upper left quadrant, where $\gamma_1 < 0$ and $\gamma_3 > 0$ is associated with the sensory cells (filled circles), whereas the other three quadrants define the cells that are non-sensory (open circles), namely, motor or complex. (C) σ_R as a function of M_R for the recorded neurons in MPC during the SCT. The black line corresponds to the best linear model between the two parameters (Pearson $r = 0.686$, $p < 0.0001$).

associated to particular task events in self-paced behaviors, such as multi-target reaching (monkey motor cortex, Cisek and Kalaska, 2005), song production (song bird auditory areas, Woolley, 2012) or foraging (rodent hippocampus, Kolling et al., 2012). Although in

these behaviors there is a set of continuous variables, such as hand velocity or body position, different landmarks or phasic events in these experiments can be used to perform our warping method.

Warping methods have been used to identify the patterns of spiking activity that are associated with specific stimuli or behavioral events, using preselected spike templates of activation (Chi et al., 2007; Lawhern et al., 2012). In contrast, our warping method determines which parameter in a sensorimotor sequence produces the lowest intertrial variability in the activity of the cell. This algorithm can be used in neural activity recorded in any cortical or subcortical structure during the execution of a sequential task, and cells in these areas can be categorized as sensory, motor, or complex using our statistical criteria. However, it is important to notice that the definition of a sensory or motor cell in the present paper depends strictly on the $L(w)$ function and the Bayes factors. Additional neurophysiological criteria, such as sensory receptive fields or the effects of microstimulation for the production of muscle contractions, are needed to define sensory or motor responses in the classical neurophysiological sense.

Bayes factors have become popular in some parts of neuroscience and psychology (see Gallistel, 2009; Lodewyckxa et al., 2011; Penny et al., 2004; Rosa et al., 2010). Although they have been used sparingly in electrophysiological studies (Cronin et al., 2010), our successful application of Bayes factors in this investigation suggests they may be of use in other neurophysiological contexts.

Acknowledgments

References

Averbeck BB, Latham PE, Pouget A. Neural correlations, population coding and computation. Nat Rev Neurosci 2006a;7:358–66.

Averbeck BB, Sohn JW, Lee D. Activity in prefrontal cortex during dynamic selection of action sequences. Nat Neurosci 2006b;9:276–82.

Baker SN, Gerstein GL. Determination of response latency and its application to normalization of cross-correlation measures. Neural Comput 2001;13:1351–77.

Chafee MV, Averbeck BB, Crowe DA. Representing spatial relationships in posterior parietal cortex: single neurons code object-referenced position. Cereb Cortex 2007;17:2914–32.

Chi Z, Wu W, Haga Z, Hatsopoulos NG, Margoliash D. Template-based spike pattern identification with linear convolution and dynamic time warping. J Neurophysiol 2007;97:1221–35.

Cisek P, Kalaska JF. Neural correlates of reaching decisions in dorsal premotor cortex: specification of multiple direction choices and final selection of action. Neuron 2005;801:14.

Cronin B, Stevenson IH, Sur M, Kording KP. Hierarchical Bayesian modeling and Markov chain Monte Carlo sampling for tuning-curve analysis. J Neurophysiol 2010;103:591–602.

Crutcher MD, Alexander GE. Movement-related neuronal activity selectively coding either direction or muscle pattern in three motor areas of the monkey. J Neurophysiol 1990;64:151–63.

Davey NJ, Ellaway PH, Stein RB. Statistical limits for detecting change in the cumulative sum derivative of the peristimulus time histogram. J Neurosci Methods 1986;17:153–66.

Ellaway P. Cumulative sum technique and its application to the analysis of peristimulus time histograms. Electroencephalogr Clin Neurophysiol 1978;45:302–4.

Gallistel CR. The importance of proving the null. Psychol Rev 2009;116:439–53.

Georgopoulos AP, Kalaska JF, Caminiti R, Massey JT. On the relations between the direction of two-dimensional arm movements and cell discharge in primate motor cortex. J Neurosci 1982;2:1527–37.

Kass RE, Raftery AE. Bayes factors. J Am Stat Assoc 1995;90:773–95.

Kolling N, Behrens TE, Mars RB, Rushworth MF. Neural mechanisms of foraging. Science 2012;336:95–8.

Lawhern V, Hatsopoulos NG, Wu W. Coupling time decoding and trajectory decoding using a target-included model in the motor cortex. Neurocomputing 2012;82:117–26.

Lee D, Port NL, Kruse W, Georgopoulos AP. Variability and correlated noise in the discharge of neurons in motor and parietal areas of the primate cortex. J Neurosci 1998;18:1161–70.

Lee D, Quessy S. Activity in the supplementary motor area related to learning and performance during a sequential visuomotor task. J Neurophysiol 2003;89:1039–56.

Liang L, Lu T, Wang X. Neural representations of sinusoidal amplitude and frequency modulations in the primary auditory cortex of awake primates. J Neurophysiol 2002;87:2237–61.

Lodewyckxa T, Kimb W, Leec MD, Tuerlinckxa F, Kuppensa P, Wagenmakers EJ. A tutorial on Bayes factor estimation with the product space method. J Math Psychol 2011;55:331–47.

Merchant H, Battaglia-Mayer A, Georgopoulos AP. Effects of optic flow in motor cortex and area 7a. J Neurophysiol 2001;86:1937–54.

Merchant H, Battaglia-Mayer A, Georgopoulos AP. Neural responses during interception of real and apparent circularly moving targets in Motor Cortex and Area 7a. Cereb Cortex 2004;14:314–31.

Merchant H, Zarco W, Prado L. Do we have a common mechanism for measuring time in the hundred of milliseconds range? Evidence from multiple interval timing tasks. J Neurophysiol 2008;99:939–49.

Merchant H, Zarco W, Perez O, Prado L, Bartolo R. Measuring time with multiple neural chronometers during a synchronization-continuation task. PNAS 2011;108:19784–9.

Mountcastle VB, Lynch JC, Georgopoulos A, Sakata H, Acuna C. Posterior parietal association cortex of the monkey: command functions for operations within extrapersonal space. J Neurophysiol 1975;38:871–908.

Mountcastle VB, Steinmetz MA, Romo R. Frequency discrimination in the sense of flutter: psychophysical measurements correlated with postcentral events in behaving monkeys. J Neurosci 1990;10:3032–44.

Nakamura K, Sakai K, Hikosaka O. Neuronal activity in medial frontal cortex during learning of sequential procedures. J Neurophysiol 1998;80:2671–87.

Nawrot MP, Aertsen A, Rotter S. Elimination of response latency variability in neuronal spike trains. Biol Cybern 2003;88:321–34.

Nowak LG, Munk MH, Girard P, Bullier J. Visual latencies in areas V1 and V2 of the macaque monkey. Vis Neurosci 1995;12:371–84.

Penny WD, Stephan KE, Mechelli A, Friston KJ. Comparing dynamic causal models. Neuroimage 2004;22:1157–72.

Repp BH. Sensorimotor synchronization: a review of the tapping literature. Psychon Bull Rev 2005;12:969–92.

Romo R, Merchant H, Zainos A, Hernández A. Categorization of somaesthetic stimuli: sensorimotor performance and neuronal activity in primary somatic sensory cortex of awake monkeys. Neuroreport 1996;7:1273–9.

Rosa MJ, Bestmann S, Harrison L, Penny W. Bayesian model selection maps for group studies. Neuroimage 2010;49:217–24.

Sanderson AC. Adaptive filtering of neuronal spike train data. IEEE Trans Biomed Eng 1980;27:271–4.

Seal J, Commenges D, Salamon R, Bioulac B. A statistical method for the estimation of neuronal response latency and its functional interpretation. Brain Res 1983;278:382–6.

Shadlen MN, Newsome WT. The variable discharge of cortical neurons: implications for connectivity, computation, and information coding. J Neurosci 1998;18:3870–96.

Tanji J. Sequential organization of multiple movements: involvement of cortical motor areas. Annu Rev Neurosci 2001;24:631–51.

Ventura V. Testing for and estimating latency effects for Poisson and non-Poisson spike trains. Neural Comput 2004;16:2323–49.

Wang K, Gasser T. Synchronization sample curves nonparametrically. Ann Statist 1999;10:1040–53.

Wing AM, Kristofferson AB. Response delays and the timing of discrete motor responses. Percept Psychophys 1973;14:5–12.

Woolley SM. Early experience shapes vocal neural coding and perception in songbirds. Dev Psychobiol 2012;54:612–31.

Zarco W, Merchant H, Prado L, Mendez JC. Subsecond timing in primates: comparison of interval production between human subjects and rhesus monkeys. J Neurophysiol 2009;102:3191–202.